Partial-State Estimation Using an Adaptive Disturbance Rejection Algorithm

Dennis S. Bernstein, Chandrasekar Jaganath, and Aaron Ridley

I. Introduction

The classical Kalman filter provides optimal least-squares estimates of all of the states of a linear time-varying system under Gaussian process and measurement noise. In many applications, however, optimal estimates are desired for a specified subset of the system states, rather than all of the system states. For example, for systems arising from discretized partial differential equations, the chosen subset of states can represent the desire to estimate state variables associated with a subregion of the spatial domain. However, the optimal state estimator for a subset of system states coincides with the classical Kalman filter.

For applications involving high-order systems, it is often difficult to implement the classical Kalman filter, and thus it is of interest to consider computationally simpler filters that yield suboptimal estimates of a specified subset of states. One approach to this problem is to consider a reduced-order Kalman filter, which provides state estimates that are suboptimal relative to the full-order Kalman filter [1–5]. Alternative variants of the classical Kalman filter have been developed for computationally demanding applications such as weather forecasting [6–11], where the classical Kalman filter gain and covariance update are modified so as to reduce the computational requirements.

The present paper is motivated by computationally demanding data assimilation applications such as those discussed in [6–9]. For such applications, a high-order simulation model is assumed to be available, and the derivation of a reduced-order filter in the sense of [1–5] is not feasible due to the lack of a tractable analytic model. We thus consider the use of a full-order state estimator based directly on the simulation model. However, we do not seek a filter gain based on the state error covariance matrix, but rather we consider an adaptive approach based on [12, 13] that depends on measurements that are available during the tuning phase. Once the tuning phase is complete, the estimator can be used to estimate the tuning-related outputs in the event that they are not available. In practice, the proposed estimator is intended for use as a faster-than-real time predictor of future values of the tuning-related outputs.

We simulate and perform state-estimation using the adaptive disturbance rejection approach on a N-mass serially interconnected mass-spring-damper system. We compare the performance of our approach with the full state Kalman filter and the spatially constrained Kalman filter. Finally, we perform state-estimation on a discretized model (first-order Roe upwind scheme) of 1-D hydrodynamic flow using the adaptive disturbance rejection approach.

This research was supported by the National Science Foundation Information Technology Research initiative, through Grant ATM-0325332 to The University of Michigan, Ann Arbor, USA.

D. S. Bernstein, C. Jaganath, and A. Ridley are with The University of Michigan, Ann Arbor, MI 48109-2140, (734) 764-3719, (734) 763-0578 (FAX), dsbaero@umich.edu

II. Spatially Constrained State Estimation

We begin by considering the discrete-time dynamical system

$$x_{k+1} = A_k x_k + B_k u_k + D_{1,k} w_k, \quad k \geq 0, \tag{2.1}$$

with output

$$y_k = C_k x_k + D_{2,k} w_k, \tag{2.2}$$

where $x_k \in \mathbb{R}^{n_k}$, $u_k \in \mathbb{R}^{m_k}$, $y_k \in \mathbb{R}^{l_k}$, and A_k, B_k, C_k are known real matrices of appropriate size. The input u_k and output y_k are assumed to be measured, and $w_k \in \mathbb{R}^{d_{k+1}}$ is zero-mean noise processes with unit variance. Define $V_{1,k} \triangleq D_{1,k} D_{1,k}^{\mathrm{T}} \in \mathbb{R}^{n_k \times n_k}$, $V_{2k} \triangleq D_{2,k} D_{2,k}^{\mathrm{T}} \in \mathbb{R}^{l_k \times l_k}$ and $V_{12k} \triangleq D_{1,k} D_{2,k}^{\mathrm{T}} \in \mathbb{R}^{n_k \times l_k}$. We assume that $V_{2,k}$ is positive definite. In discretized PDE models, the dimension of the state varies at every step depending on the desired resolution. To encompass such applications we let the dimension n_k of the state x_k be time varying, and thus $A_k \in \mathbb{R}^{n_{k+1} \times n_k}$ is not necessarily square.

For the system (2.1) and (2.2), we consider a state estimator of the form

$$\hat{x}_{k+1} = A_k \hat{x}_k + B_k u_k + \Gamma_k K_k (y_k - \hat{y}_k), \tag{2.3}$$

with output

$$\hat{y}_k = C_k \hat{x}_k, \tag{2.4}$$

where $\hat{x}_k \in \mathbb{R}^{n_k}$, $\hat{y}_k \in \mathbb{R}^{l_k}$, $\Gamma_k \in \mathbb{R}^{n_{k+1} \times p_k}$, and $K_k \in \mathbb{R}^{p_k \times l_k}$. The nontraditional feature of (2.3) is the presence of the term Γ_k, which, in the classical output injection case is the identity matrix. Here, Γ_k constrains the state estimator so that only states in the range of Γ_k are directly affected by the the gain K_k. For example, Γ_k can have the form $\Gamma_k = \left[\begin{array}{ccc} 0 & I_{p_k} & 0 \end{array} \right]^{\mathrm{T}}$, where I_r denotes the $r \times r$ identity matrix. We assume that Γ_k has full column rank for all $k \geq 0$.

Next, define the state estimation error $e_k \triangleq x_k - \hat{x}_k$, and define the cost function

$$J_k(K_k) \triangleq \mathcal{E}[(L_k e_{k+1})^{\mathrm{T}} L_k e_{k+1}], \tag{2.5}$$

where $\mathcal{E}[\cdot]$ denotes expected value and $L_k \in \mathbb{R}^{q_k \times n_{k+1}}$

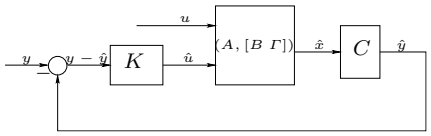

Fig. 1. State estimator cast as a feedback controller in a servo loop

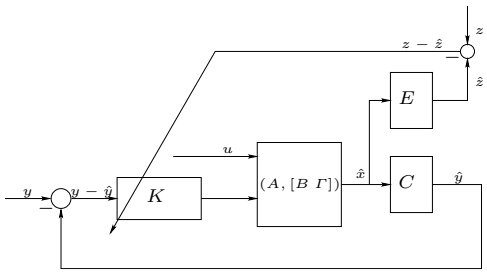

Fig. 2. Adaptive partial-state estimator using the performance error for controller tuning

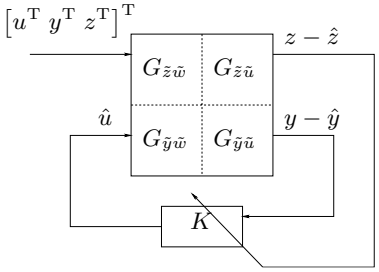

Fig. 3. Partial state estimation problem using the performance error $z-\hat{z}$ for controller tuning recast as a standard problem.

determines the weighting on the components of the error.

Under the given assumptions and in the case in which Γ_k is the identity matrix, the minimum covariance controller is given by the classical Kalman filter. For the case in which $\Gamma_k \neq I$ it can be shown that the filter gain K_k that minimizes J_k in (2.5) is given by

$$K_k = (\Gamma_k^{\mathrm{T}} M_k \Gamma_k)^{-1} \Gamma_k^{\mathrm{T}} M_k \hat{V}_{12,k} \hat{V}_{2,k}^{-1}, \tag{2.6}$$

where $M_k \triangleq L_k^{\mathrm{T}} L_k$, and $\hat{V}_{2,k} \in \mathbb{R}^{l_k \times l_k}$ and $\hat{V}_{12,k} \in \mathbb{R}^{n_k \times l_k}$ are defined by

$$\hat{V}_{2,k} \triangleq V_{2,k} + C_k Q_k C_k^{\mathrm{T}},\ \hat{V}_{12,k} \triangleq V_{12,k} + A_k Q_k C_k^{\mathrm{T}}. \tag{2.7}$$

The error covariance Q_k is updated using

$$\begin{aligned} Q_{k+1} = A_k Q_k A_k^{\mathrm{T}} + \pi_{k\perp} \hat{V}_{12,k} \hat{V}_{2,k}^{-1} \hat{V}_{12,k}^{\mathrm{T}} \pi_{k\perp}^{\mathrm{T}} \\ + V_{1,k} - \hat{V}_{1,k} \hat{V}_{2,k}^{-1} \hat{V}_{12,k}^{\mathrm{T}}, \end{aligned} \tag{2.8}$$

where $\pi_k \in \mathbb{R}^{n_{k+1} \times n_{k+1}}$ is defined by

$$\pi_k \triangleq \Gamma_k (\Gamma_k^{\mathrm{T}} M_k \Gamma_k)^{-1} \Gamma_k^{\mathrm{T}} M_k. \tag{2.9}$$

and the complementary projector $\pi_{k\perp}$ is defined by $\pi_{k\perp} \triangleq I_n - \pi_k$. Note that both the optimal filter gain K_k in (2.6) and the classical Kalman filter gain depend on the state covariance matrix, which is propagated by means of a Riccati equation update. For large scale systems, this update is computationally demanding, and we thus seek an alternative approach to state estimation.

To motivate the adaptive partial-state estimator discussed in the following section, we illustrate the Kalman filter structure in the form of the closed-loop system shown in Figure 1, where, for simplicity, we omit the time dependence. We first note that the feedback gain K represents a MIMO, memoryless controller, that is, a proportional controller, which can be time varying. Since Figure 1 shows a basic servo loop, classical design considerations suggest that high gain improves performance subject to stability considerations. In fact, a high gain K suppresses the magnitude of $y - \hat{y}$, although this performance metric will not necessarily yield optimal state estimates.

The classical Kalman filter chooses a feedback gain K that provides optimal estimates of every state rather than a minimum value of the magnitude of $y - \hat{y}$. This tuning is achieved based on knowledge of the state estimate error as determined online by means of the Riccati update of the covariance. Alternatively, a feedback gain K can be designed by means of standard control techniques that do not require propagation of the state covariance. In this approach, the controller does not provide an optimal estimate of the entire state, but rather an estimate of only states (or combinations of states) modeled by z. For example, if (2.1) is a linear time-invariant system, then LQG theory can be used to obtain a feedback controller in the form of a full-order dynamic compensator with y modeled as the output of a dynamical system driven by white noise. This approach, however, is computationally demanding and fails to exploit the information obtained from measurements of z.

III. Adaptive Partial-State Estimation

In this section, we propose an adaptive approach to tuning the state-estimator feedback controller K in Figure 1. Consider a linear time-invariant system with dynamics given by

$$x_{k+1} = Ax_k + Bu_k + D_1 w_k, \tag{3.1}$$

and output

$$y_k = Cx_k + Du_k + D_2 w_k, \tag{3.2}$$

where $x_k \in \mathbb{R}^n$, $u_k \in \mathbb{R}^m$, and $y_k \in \mathbb{R}^l$. The input u_k and output y_k are assumed to be measured, and $w_k \in \mathbb{R}^d$ is zero-mean noise process with unit variance. Next, define $z_k \in \mathbb{R}^q$ by

$$z_k = E_1 x_k + E_2 u_k + E_0 w_k \tag{3.3}$$

This approach is based on the signal z in (3.3) that is assumed to be available for tuning. The objective of the estimator is to provide an estimate of z when measurements of z are not available such as in future prediction. The signal z can be a subset of the signal y, or it can be an additional signal. The adaptive partial state estimation problem is shown in Figure 2. We assume that y_k is available for all

$k \geqslant 0$ and z_k is available for all $0 \leqslant k \leqslant k_0$, where $k_0 > 0$.

Consider an estimator with dynamics

$$\begin{aligned} \hat{x}_{k+1} &= A\hat{x}_k + Bu_k + \Gamma\hat{u}_k, \\ \hat{y}_k &= C\hat{x}_k + Du_k, \\ \hat{z}_k &= E_1\hat{x}_k. \end{aligned} \tag{3.4}$$

The innovations term usually found in the Kalman filter is incorporated in the controller output $\hat{u}_k \in \mathbb{R}^p$. As mentioned in Section 2, $\Gamma \in \mathbb{R}^{n\times p}$ determines the state estimates that are directly affected by $\hat{u}_k$. The controller K is tuned using $z_k - \hat{z}_k$ for $k \leqslant k_0$, and the tuned controller is then be used to produce estimates $\hat{z}_k$ of z_k for all $k > k_0$.

The problem in Figure 2 is recast as the standard problem in Figure 3. Define $\tilde{w}_k$, $\tilde{u}_k$, $\tilde{y}_k$ and $\tilde{z}_k$ by

$$\begin{aligned} \tilde{w}_k &\triangleq \left[\begin{array}{c} u_k \\ y_k \\ z_k \end{array}\right], \quad \tilde{u}_k \triangleq \hat{u}_k, \\ \tilde{y}_k &\triangleq y_k - \hat{y}_k, \qquad \tilde{z}_k \triangleq z_k - \tilde{z}_k. \end{aligned} \tag{3.5}$$

It then follows from (3.1)-(3.5) that

$$\left[\begin{array}{c} \tilde{z} \\ \tilde{y} \end{array}\right] = \mathcal{G}\left[\begin{array}{c} \tilde{w} \\ \tilde{u} \end{array}\right], \tag{3.6}$$

where $\mathcal{G}$ has the realization

$$\mathcal{G} \sim \left[\begin{array}{c|c:c} \mathcal{A} & \mathcal{D}_1 & \mathcal{B} \\ \hline \mathcal{E}_1 & 0 & \mathcal{E}_2 \\ \hdashline \mathcal{C} & \mathcal{D}_2 & \mathcal{D} \end{array}\right] \tag{3.7}$$

with state $\hat{x}$ and

$$\begin{aligned} &\mathcal{A} \triangleq A, \quad \mathcal{B} \triangleq \Gamma, \quad \mathcal{D}_1 \triangleq \left[\begin{array}{ccc} B & 0 & 0 \end{array}\right], \\ &\mathcal{C} \triangleq -C, \quad \mathcal{D} \triangleq 0, \quad \mathcal{D}_2 \triangleq \left[\begin{array}{ccc} 0 & I & 0 \end{array}\right], \\ &\mathcal{E}_1 \triangleq -E_1, \quad \mathcal{E}_2 \triangleq 0, \quad \mathcal{E}_0 \triangleq \left[\begin{array}{ccc} 0 & 0 & I \end{array}\right]. \end{aligned} \tag{3.8}$$

It follows from (3.7) and (3.8) that

$$\mathcal{G} = \left[\begin{array}{cc} G_{\tilde{z}\tilde{w}} & G_{\tilde{z}\tilde{u}} \\ G_{\tilde{y}\tilde{w}} & G_{\tilde{y}\tilde{u}} \end{array}\right] \tag{3.9}$$

where

$$\begin{aligned} &G_{\tilde{z}\tilde{w}} \triangleq \left[\begin{array}{ccc} -G_{E,B} & 0 & I \end{array}\right], \quad G_{\tilde{z}\tilde{u}} \triangleq -G_{E,\Gamma}, \\ &G_{\tilde{y}\tilde{w}} \triangleq \left[\begin{array}{ccc} -G_{C,B} & I & 0 \end{array}\right], \quad G_{\tilde{z}\tilde{u}} \triangleq -G_{C,\Gamma} \end{aligned} \tag{3.10}$$

and $G_{E,B}$, $G_{E,\Gamma}$, $G_{C,B}$, and $G_{C,\Gamma}$ denote the systems (A, B, E), (A, Γ, E), (A, B, C) and (A, Γ, C), respectively. The objective of the adaptive disturbance rejection problem is to minimize $\|\tilde{z}_k\| = \|z_k - \hat{z}_k\|$. Note that $\tilde{z}_k$ is available only for all $k \leqslant k_0$ and, since y_k is available for all $k > 0$, it follows from (3.2), (3.4) and (3.5) that $\tilde{y}_k$ is also available for all $k \geqslant 0$.

IV. The Adaptive Time-Series Controller

The dynamic compensator K is tuned using an adaptive algorithm that uses current and past measurements of $\tilde{z}_k$ and $\tilde{u}_k$ defined in (3.5). The adaptive algorithm uses the Markov parameters from the controller output $\tilde{u}_k$ to the performance variable $\tilde{z}_k$ in a time-series controller framework [13]. The Markov parameters are assumed to be known. It follows from (3.6)-(3.8) that, for $i = 0, 1, \ldots$, the Markov parameters $H_i \in \mathbb{R}^{q\times p}$ from the control $\tilde{u}_k$ to the performance variable $\tilde{z}_k$ are given by

$$H_i = \begin{cases} \mathcal{E}_2 = 0, & \text{if } i = 0, \\ \mathcal{E}_1\mathcal{A}^{i-1}\mathcal{B} = -E_1A^{i-1}\Gamma, & \text{if } i \geqslant 1. \end{cases} \tag{4.1}$$

Next, define $\mathcal{H} \in^{qp_c\times p(p_c+q_c)}$ by

$$\mathcal{H} \triangleq \left[\begin{array}{ccccccc} H_0 & \cdots & H_{q_c} & 0_{q\times p} & \cdots & 0_{q\times p} \\ 0_{q\times p} & \ddots & & \ddots & \ddots & \vdots \\ \vdots & \ddots & \ddots & & \ddots & 0_{q\times p} \\ 0_{q\times p} & \cdots & 0_{q\times p} & H_0 & \cdots & H_{q_c} \end{array}\right], \tag{4.2}$$

where the positive integers p_c and q_c are the controller parameters that determine the order of the dynamic controller K. Next, define $\Phi_{uy,k} \in \mathbb{R}^{(p+l)(n_c+q_c+p_c-1)}$, $Z_k \in \mathbb{R}^{qp_c}$ and $U_k \in \mathbb{R}^{p(p_c+q_c)}$ by

$$\Phi_{uy,k} \triangleq \left[\begin{array}{c} \hat{u}_{k-1} \\ \vdots \\ \hat{u}_{k-n_c-q_c-p_c+1} \\ \tilde{y}_{k-1} \\ \vdots \\ \tilde{y}_{k-n_c-q_c-p_c+1} \end{array}\right], Z_k \triangleq \left[\begin{array}{c} \tilde{z}_k \\ \vdots \\ \tilde{z}_{k-p_c+1} \end{array}\right], U_k \triangleq \left[\begin{array}{c} \hat{u}_k \\ \vdots \\ \hat{u}_{k-p_c-q_c+1} \end{array}\right]. \tag{4.3}$$

For all $i = 1, \ldots, q_c + p_c$, define $L_i \in \mathbb{R}^{p(p_c+q_c)\times p}$ by

$$L_i \triangleq \left[\begin{array}{c} 0_{(i-1)p\times p} \\ I_p \\ 0_{(p_c+q_c-i)p\times p} \end{array}\right] \tag{4.4}$$

and $R_i \in \mathbb{R}^{n_c(p+l)\times(n_c+p_c+q_c-1)(p+q)}$ by

$$R_i \triangleq \left[\begin{array}{ccccc} R_{i,11} & R_{i,12} & R_{i,13} & R_{i,14} & R_{i,15} \\ R_{i,21} & R_{i,22} & R_{i,23} & R_{i,24} & R_{i,25} \end{array}\right], \tag{4.5}$$

where

$$\begin{aligned} &R_{i,11} = 0_{n_cp\times(i-1)p}, && R_{i,12} = I_{n_cp}, \\ &R_{i,13} = 0_{n_cp\times((p_c+q_c-i)p+(i-1)l)}, && R_{i,14} = 0_{n_cp\times n_cl}, \\ &R_{i,15} = 0_{n_cp\times(p_c+q_c-i)l}, && R_{i,21} = 0_{n_cl\times(i-1)p}, \\ &R_{i,23} = 0_{n_cl\times((p_c+q_c-i)p+(i-1)l)}, && R_{i,22} = 0_{n_cl\times(i-1)p}, \\ &R_{i,25} = 0_{n_cl\times(p_c+q_c-i)l}, && R_{i,24} = I_{n_cl}. \end{aligned} \tag{4.6}$$

The adaptive control law given in [13] has the form

$$\hat{u}_k = \Theta_k R_1 \Phi_{uy,k}, \tag{4.7}$$

where the controller Θ_k is updated using

$$\Theta_{k+1} = \Theta_k - \eta_k \frac{\partial J_k}{\partial \Theta_k}. \tag{4.8}$$

The gradient $\frac{\partial J_k}{\partial \Theta_k}$ and the adaptive step size η_k are given by

$$\begin{aligned} \frac{\partial J_k}{\partial \Theta_k} &\triangleq \sum_{i=1}^{q_c+p_c} L_i^{\mathrm{T}}\mathcal{H}^{\mathrm{T}}\hat{Z}_k\Phi_{uy,k}^{\mathrm{T}}R_i^{\mathrm{T}}, \\ \eta_k &\triangleq \frac{1}{(p_c+q_c)\,\|\mathcal{H}\|_{\mathrm{F}}^2\|\Phi_{uy,k}\|_2^2}, \end{aligned} \tag{4.9}$$

where $\hat{Z}_k \triangleq Z_k - \mathcal{H}U_k + \mathcal{H}\sum_{i=1}^{p_c+q_c} L_i\Theta_kR_i\Phi_{uy,k}$.

Assume that an event of interest occurs at $k = k_0$, and that the signal z_k is unavailable for $k > k_0$. The controller Θ_k is updated for $0 \leqslant k \leqslant k_0$ using (4.8). For $k > k_0$, $\tilde{z}_k$ is unavailable and hence the controller cannot be tuned using (4.8). Instead, for all $k > k_0$, the tuned controller Θ_{k_0} is used in (4.7) to produce $\hat{u}_k$ that minimizes $\|\tilde{z}_k\|$.

V. N-Mass System Example

Consider the N-mass serially interconnected system shown in the Figure 4. For all $i = 1, \ldots, N$, let $x_{\mathrm{pos},i}$

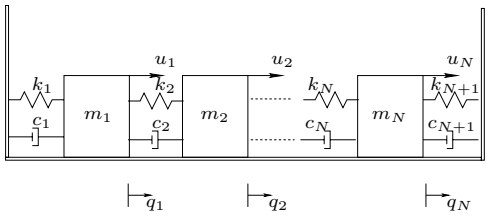

Fig. 4. N-Mass System

and $x_{\mathrm{vel},i}$ be the position and velocity of the ith mass, respectively. The plant dynamics are given by (3.1)-(3.3), where the state x is defined by

$$x \triangleq \begin{bmatrix} x_{\mathrm{pos},1} & x_{\mathrm{vel},1} & \cdots & x_{\mathrm{pos},N} & x_{\mathrm{vel},N} \end{bmatrix}^{\mathrm{T}} \tag{5.1}$$

and, A, B, C, and E_1 in (3.1)-(3.3) are obtained using a zero-order hold discretization of the continuous-time model of the mass-spring-damper system.

Assume that $N = 10$ so that the system is of order $n = 20$. The forcing $u_k \in \mathbb{R}^2$ on m_1 and m_3 is assumed to be a multi-tonal sinusoidal signal and is available for all $k > 0$. The forcing $w_{1k} \in \mathbb{R}^2$ on m_2 and m_4 is assumed to be zero-mean noise with unit covariance and is unavailable for all $k > 0$. Measurement y_k of the positions of m_5 and m_6 is available for all k and measurement z_k of the positions of m_7 and m_8 is available only for $k \leqslant k_0$ ($k_0 = 1000$). The objective is to estimate the position of m_7 and m_8 for all $k > k_0$. The sensor noise $w_{2k} \in \mathbb{R}^2$ and $w_{3k} \in \mathbb{R}^2$, corresponding to measurements y_k and z_k, respectively are assumed to be zero-mean noise with unit covariance so that w_k defined in (3.1) is given by $w_k = \begin{bmatrix} w_{1k}^{\mathrm{T}} & w_{2k}^{\mathrm{T}} & w_{3k}^{\mathrm{T}} \end{bmatrix}^{\mathrm{T}}$ for $k \leqslant k_0$.

The estimates from the adaptive disturbance rejection algorithm are obtained using (3.4), where $\hat{u}_k$ is produced by the adaptive controller described in Section 4. Furthermore, we choose $\Gamma = E_1^{\mathrm{T}}$. Since measurements of z_k and y_k are available for $k \leqslant k_0$, (3.4) is used to evaluate $\tilde{z}_k$ and $\tilde{y}_k$ to tune the controller using (4.3)-(4.9). After $k > k_0$, measurements of z_k are unavailable and the tuned controller Θ_{k_0} is used in (4.7) to produce $\hat{u}_k$ that affects the estimate of the position of m_7 and m_8 through Γ. The controller is initialized with $\Theta_0 = 0$, and we choose $n_c = 10$, $p_c = 6$ and $q_c = 8$.

The state estimates from the spatially constrained Kalman filter are obtained using (2.3) and (2.4) with $A_k = A$, $B_k = B$, for $k \geqslant 0$. However, since z_k is available only for $0 \leqslant k \leqslant k_0$, C_k in (2.4) is given by

$$C_k = \begin{cases} \begin{bmatrix} C^{\mathrm{T}} & E_1^{\mathrm{T}} \end{bmatrix}^{\mathrm{T}}, & \text{if } 0 \leqslant k \leqslant k_0, \\ C, & \text{if } k > k_0. \end{cases} \tag{5.2}$$

To compare the estimates obtained from the spatially constrained Kalman filter with those from the adaptive disturbance rejection estimator, we choose Γ in (2.3) so that only the estimates of position of m_7 and m_8 are in the range of Γ. Furthermore, we let $L_k = \Gamma^{\mathrm{T}}$ so that only the error in the estimates of position of m_7 and m_8 are weighted in (2.5).

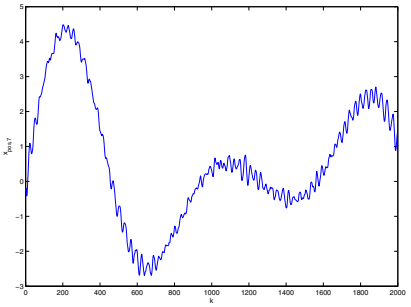

Fig. 5. The actual position of m_7 is shown in this figure.

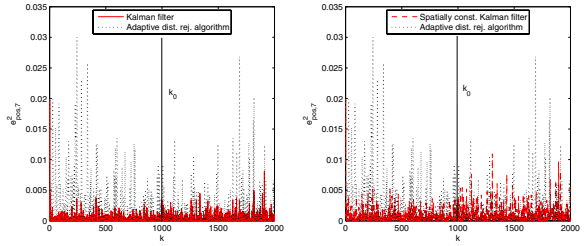

Fig. 6. The square of the error between the actual position of m_7 and the estimates obtained from the three methods, namely, Kalman filter, spatially constrained Kalman filter and the adaptive disturbance rejection estimator. State estimation is the performance objective only after $k > k_0$

Figure 5 shows $x_{\mathrm{pos},7}$, the actual position of m_7, when forced by a sinusoidal input and Gaussian process noise. The square of the error between the actual position of m_7 and the state estimates is plotted in Figure 6.

Next, we consider the adaptive disturbance rejection estimator when the input u_k is unavailable. Assume that the forcing u_k on the mass m_1 and m_3 is available only for $0 \leqslant k \leqslant k_{\mathrm{inp}}$ and not available for $k > k_{\mathrm{inp}}$. For $k \leqslant k_{\mathrm{inp}}$, the estimator dynamics and the standard problem is given by (3.4)-(3.8). For all $k > k_{\mathrm{inp}}$, the estimator dynamics are given by (3.4)-(3.8) with $B = 0$ and $D = 0$. Since u_k does not appear in (4.3)-(4.9), the adaptive disturbance rejection algorithm does not depend on the availability of u_k. Furthermore, it follows from (3.8), and (4.1) that the Markov parameters required for the adaptive disturbance rejection algorithm are the same whether u_k is available or not.

Note that both the Kalman filter and the spatially constrained Kalman filter described in Section 2 require that the plant input u_k in (3.1)-(3.3) be known for $k \geqslant 0$. If u_k is unavailable for all $k > k_{\mathrm{inp}}$, the estimator dynamics of the spatially constrained Kalman filter is given by (2.3) with $A_k = A$,

$$B_k = \begin{cases} B, & \text{if } 0 \leqslant k \leqslant k_{\mathrm{inp}}, \\ 0, & \text{if } k > k_{\mathrm{inp}}. \end{cases} \tag{5.3}$$

and C_k given by (5.2).

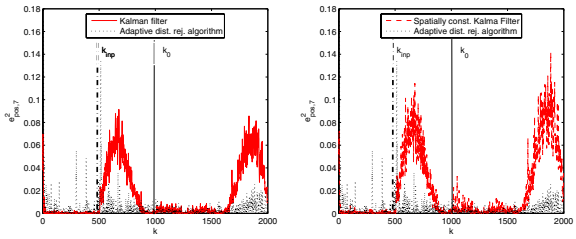

Fig. 7. Error in the state estimates using the Kalman filter, spatially constrained Kalman filter and the adaptive disturbance rejection estimator. The original mass-spring-damper system is of order $n = 20$, however the adaptive controller of order $n_c = 2$ yields better estimates of $x_{7,\mathrm{pos}}$ than the Kalman filter and the spatially constrained Kalman filter.

The Kalman filter and the spatially constrained Kalman filter propagate the state error covariance at every time step. Since $n = 20$ in our example, $Q_k \in \mathbb{R}^{20\times 20}$ in (2.8) irrespective of the number of states we need to estimate. However, the order n_c of the adaptive controller can be chosen smaller than n so that the computational burden of using the adaptive disturbance rejection controller is lower than the spatially local Kalman filtering approach. Figure 7 shows the error in estimate of the position of m_7 from the adaptive disturbance rejection algorithm when a lower order controller of order $n_c = 2$ is used. The error in estimates obtained from the Kalman filter and the spatially constrained Kalman filter are also shown in the same figure. The total time taken to perform data assimilation using the adaptive disturbance rejection estimator is about 6% less than the time taken by the spatially constrained Kalman filter, when both estimators are simulated for $k = 0, \ldots, 2000$. In all three estimation techniques, the input u_k is assumed to be unknown for $k > k_{\mathrm{inp}}$.

VI. 1-D Hydrodynamic Flow Example

Next, we apply the adaptive disturbance rejection estimator for state estimation of hydrodynamic flow. Consider a one dimensional compressible and inviscid flow. The flow dynamics involving PDE's are given by Euler's equations. A finite-volume discrete-time model of the hydrodynamic flow can be obtained using the upwind Roe's scheme. Assuming Neumman boundary conditions at the first cell and Dirichlet boundary condition at the last cell, it follows from [14] that the state update equation is

$$x_{k+1} = f(x_k, u_{\mathrm{BC},k} + w_{\mathrm{BC},k}), \tag{6.1}$$

where $x \in \mathbb{R}^{3(n-2)}$ and $u_{\mathrm{BC}} \in \mathbb{R}^3$ are defined by

$$\begin{aligned} x &\triangleq \begin{bmatrix} \varrho_2 & m_2 & \mathcal{E}_1 & \cdots & \varrho_{n-1} & m_{n-1} & \mathcal{E}_{n-1} \end{bmatrix}^{\mathrm{T}}, \\ u_{\mathrm{BC}} &\triangleq \begin{bmatrix} \varrho_1 & m_1 & \mathcal{E}_1 \end{bmatrix}^{\mathrm{T}} \end{aligned} \tag{6.2}$$

and for $i = i, \ldots, n$, ϱ_i, m_i, and $\mathcal{E}_i \in \mathbb{R}$ are the density, momentum, and energy, at the center of the ith cell (indicated by the black dots in Figure 8), respectively. The structure of $f(\cdot)$ in (6.1) is defined in [14] and involves the difference in the values of the flow variables at the edge of the cells (indicated by the white dots). Note that $u_{\mathrm{BC},k}$ is the boundary condition at the first cell and is assumed to be known, however $w_{\mathrm{BC},k} \in \mathbb{R}^3$ represents the unmodeled drivers and is unavailable for all $k \geqslant 0$. The nonlinear discrete-time update equation (6.1) can be expressed as

$$x_{k+1} = A(x_k)x_k + B(x_k, u_{\mathrm{BC},k} + w_{\mathrm{BC},k}), \tag{6.3}$$

so that (6.3) resembles a frozen-in-time state dependent linear equation. Note that the parametrization of $A(x_k)$ and $B(x_k, u_{\mathrm{BC},k} + w_{\mathrm{BC},k})$ is not unique. Let y_k and z_k be the measurements of density, momentum and energy at certain cells so that

$$\begin{aligned} y_k &= Cx_k + D_2 w_k, \\ z_k &= E_1 x_k + E_0 w_k, \end{aligned} \tag{6.4}$$

where w_k is the sensor noise with zero-mean and unit covariance. Note that entries of C and E_1 are either 1's or 0's depending on the cells where measurements are available.

Let $n = 20$ so that $x \in \mathbb{R}^{54}$. For all $k \geqslant 0$, the boundary condition at the first cell is given by

$$u_{\mathrm{BC},k} = \begin{bmatrix} \varrho_{1,k} \\ m_{1,k} \\ \mathcal{E}_{1,k} \end{bmatrix} = \begin{bmatrix} 1 \\ 12 + \sin(20k) \\ 87 + 0.5\sin^2(20k) + 12\sin(20k) \end{bmatrix}. \tag{6.5}$$

Assume that the unmodeled driver w_{BC} is zero-mean noise with unit covariance. Let $y_k \in \mathbb{R}^6$ be the measurements of density, momentum and energy at the 5th and 10th cell, and let $z_k \in \mathbb{R}^3$ be the measurements of density, momentum and energy at the 19th cell. Assume that the measurement y_k is available for all $k > 0$, and measurement z_k is only available only for $0 \leqslant k \leqslant k_0$. The objective is to estimate the density, momentum and energy at the cells determined by E_1 when measurements of z_k are unavailable.

Consider an estimator of the form

$$\begin{aligned} \hat{x}_{k+1} &= A(\hat{x}_k)\hat{x}_k + B(\hat{x}_k, u_{\mathrm{BC},k}) + \Gamma\hat{u}_k, \\ \hat{y}_k &= C\hat{x}_k, \\ \hat{z}_k &= E_1\hat{x}_k, \end{aligned} \tag{6.6}$$

where $\hat{u}_k$ is produced by an adaptive controller. Furthermore, we choose $\Gamma = E_1^{\mathrm{T}}$ so that only the estimates of the cell whose measurements we need to estimate are directly affected by $\hat{u}_k$ through Γ in (6.6). Note that the adaptive time-series controller described in Section 4 requires the Markov parameters defined in (4.1). However, (6.1) is a nonlinear system and hence, for $i = 0, 1, \ldots$, we define the state-dependent Markov parameters $H(\hat{x}_k)_i$ by

$$H_{k,i} = \begin{cases} 0, & \text{if } i = 0, \\ -E_1 A(\hat{x}_{k-1}) \cdots A(\hat{x}_{k-i+1})\Gamma, & \text{if } i \geqslant 1. \end{cases} \tag{6.7}$$

Define $\mathcal{H}_k$ by (4.2) with H_i replaced by $H_{k,i}$. The adaptive disturbance rejection algorithm is then given by (4.3)-(4.9) with $\mathcal{H}$ replaced by $\mathcal{H}_k$. Since measurements of the density, momentum and pressure at the 5th and 10th cell (y_k), and 19th cell (z_k) are available for $k \leqslant k_0$ (k_0 = 500), (3.4) is used to evaluate $\tilde{z}_k$ and $\tilde{y}_k$ to tune the controller using the adaptive disturbance rejection algorithm with state-dependent Markov parameters. After $k > k_0$, measurements

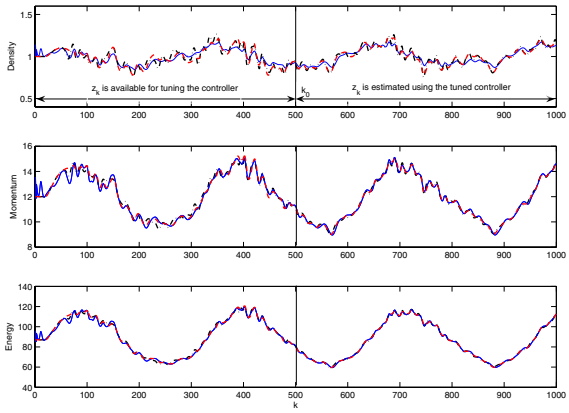

Fig. 8. State estimate using the adaptive disturbance rejection estimator that uses the state dependent Markov parameters. The estimates obtained with $n_c = 10$ and $\Gamma = E_1^{\mathrm{T}}$ are shown by dashed-dot lines $(-\cdot)$. The estimates obtained from the adaptive disturbance rejection estimator with $n_c = 15$ and $\Gamma = \tilde{\Gamma}$ are shown by dashed lines $(--)$. The actual values of density, momentum and energy at the 19th cell are shown by solid lines.

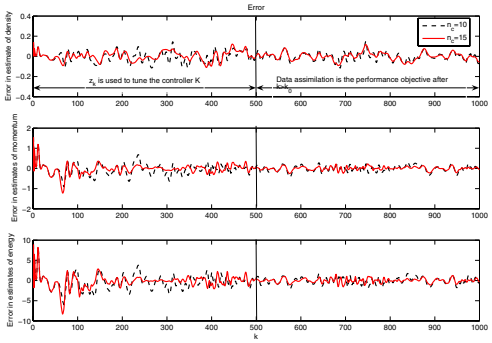

Fig. 9. The error between the actual density, momentum and energy at the 19th cell and the estimates obtained from the adaptive disturbance rejection estimator with $n_c = 10$ and $n_c = 15$.

of z_k are unavailable and the tuned controller is used to produce $\hat{u}_k$ in (6.6). The controller is initialized with $\Theta_0 = 0$, and we choose $n_c = 10$, $p_c = 8$ and $q_c = 8$.

Figure 9 shows the actual density, momentum and energy at the 19th cell and the estimates obtained using the adaptive disturbance rejection estimator that uses the state-dependent Markov parameters. The estimate of the density at the 19th cell is quite poor, however the estimates of the momentum and energy at the 19th cell are accurate.

Next, we evaluate the performance of the adaptive disturbance rejection estimator when a higher order controller is used and more states are directly affected by $\hat{u}_k$ through Γ. We choose $\Gamma = \tilde{\Gamma}$, so that the estimates of density, momentum and energy at cells 17-19 are directly affected by $\hat{u}_k$ through Γ in (6.6). Furthermore, we use a higher order controller with $n_c = 15$ to obtain the state estimates at the 19th cell. The error in the estimates at the 19th cell obtained using the adaptive disturbance rejection estimator with $n_c = 10$ and $\Gamma = E_1^{\mathrm{T}}$, and with $n_c = 15$ and $\Gamma = \tilde{\Gamma}$ are shown in Figure 10.

VII. Conclusion

In this paper, we develop an adaptive disturbance rejection framework to achieve partial state estimation. The cost of covariance propagation in the Kalman filter and the spatially local Kalman filter is prohibitive if the order of the system is large. Alternatively, the order of the adaptive controller can be chosen manually and the adaptive disturbance rejection algorithm yields better estimates in the presence of large uncertainty in the plant inputs. The state estimation using the adaptive disturbance rejection technique was demonstrated on a serially interconnected mass spring damper simulation example and its performance compared with the Kalman filter. The adaptive disturbance rejection estimator that uses the state dependent Markov parameters was then used for data assimilation in a one dimensional hydrodynamic flow example.

References

[1] D. S. Bernstein and D. C. Hyland, "The Optimal Projection Equations for Reduced-Order State Estimation," *IEEE Trans. Autom. Contr.*, Vol. AC-30, pp. 583-585, 1985.

[2] P. Hippe and C. Wurmthaler, "Optimal Reduced-Order Estimators in the Frequency Domain: The Discrete-Time Case," *Int. J. Contr.*, Vol. 52, pp. 1051-1064, 1990.

[3] W. M. Haddad and D. S. Bernstein, "Optimal Reduced-Order Observer-Estimators," *AIAA J. Guid. Dyn. Contr.,* Vol. 13, pp. 1126-1135, 1990.

[4] W. M. Haddad, D. S. Bernstein, H.-H. Huang, and Y. Halevi, "Fixed-Order Sampled-Data Estimation," *Int. J. Contr.*, Vol. 55, pp. 129-139, 1992.

[5] C.-S. Hsieh, "The Unified Structure of Unbiased Minimum-Variance Reduced-Order Filters," *Proc. Contr. Dec. Conf.*, pp. 4871-4876, Maui, HI, December 2003.

[6] B. F. Farrell and P. J. Ioannou, "State Estimation Using a Reduced-Order Kalman Filter," *J. Atmos. Sci.*, Vol. 58, pp. 3666-3680, 2001.

[7] A. W. Heemink, M. Verlaan, and A. J. Segers, "Variance Reduced Ensemble Kalman Filtering," *Mon. Weather Rev.*, Vol. 129, pp. 1718-1728, 2001.

[8] J. Ballabrera-Poy, A. J. Busalacchi, and R. Murtugudde, "Application of a Reduced-Order Kalman Filter to Initialize a Coupled Atmosphere-Ocean Model: Impact on the Prediction of El Nino," *J. Climate*, Vol. 14, pp. 1720-1737, 2001.

[9] P. Fieguth, D. Menemenlis, and I. Fukumori, "Mapping and Pseudo-Inverse Algorithms for Data Assimilation," *Proc. Int. Geoscience Remote Sensing Symp.*, pp. 3221-3223, 2002.

[10] D. I. Lawrie, P. J. Fleming, G. W. Irwin, and S. R. Jones, "Kalman Filtering: A Survey of Parallel Processing Alternatives," *Proc. IFAC Workshop on Algorithms and Architectures for Real-Time Control*, pp. 49-56, 1992, Pergamon.

[11] A. Asif and J. M. F. Moura, "Data Assimilation in Large Time-Varying Multidimensional Fields," *IEEE Trans. Image Processing*, Vol. 8, pp. 1593-1607, 1999.

[12] R. Venugopal and D. S. Bernstein, "Adaptive Disturbance Rejection Using ARMARKOV/Toeplitz Models," *IEEE Trans. Contr. Sys. Tech.*, vol. 8, pp. 257-269, 2000.

[13] J. B. Hoagg and D. S. Bernstein, "Discrete-Time Adaptive Feedback Disturbance Rejection Using a Retrospective Performance Measure," *Proc. ACTIVE 04*, Williamsburg, VA, September 2004.

[14] C. Hirsch, *Numerical Computation of Internal and External Flows,* pp. 408-469, John Wiley and Sons, 1994.